

On Coupling of Interface and Phase-field Damage Models for Quasi-brittle Fracture

Roman Vodička^{1,*}

¹ Technical University of Košice, Faculty of Civil Engineering, Vysokoškolská 4, 042 00 Košice, Slovakia

Abstract: Numerical simulations of crack initiation and propagation is presented. Both, interface and material cracks are modelled within the damage theory introducing two independent damage parameters. The interface cracks appearing in an adhesive layer of a contact zone between structural components consider cohesive zone models with general stress-strain relationships implemented in an energetic formulation. Accordingly, the fracture of bulk domains also includes variational consideration and leads to phase-field damage which causes a very narrow band of defected material constituting the actual crack. The proposed computational approach has a variational form, the solution being approximated by a time stepping procedure, a finite element code, and quadratic programming algorithms.

Keywords: *interface crack; diffuse crack; numerical simulation; staggered scheme; quadratic programming.*

1. Introduction

Damage of engineering constructions may lead in many cases to forming of cracks. Such cracks then modify mechanical and other characteristics of structures. Efficient computational algorithms for analysing and predicting such situations are highly appreciated as they may reduce production and operation costs of constructions and machines. The arising cracks may have various origin, but basically, they appear either inside material domains or along material interfaces, e.g. adhesive joints or contacts. If a crack in the material forms first, after its propagation it may hit an interface and later continue growing along it. Also, an opposite situation is possible, when a primary interface crack kinks into the bulk. The present approach can study both situations.

The proposed model interprets cracks in terms of damage mechanics where the situation in the structure, concerning e.g. density of micro-cracks or micro-voids, is described by internal variables [1,2] which reflect the state of material or adhesive degradation, and reaching their limit value means a new crack formation or existing crack propagation.

As other nonlinear phenomena, damage and fracture can be treated in terms of energies stored or dissipated from the structure allowing for a variational solution technique. Author's previous outputs [3,4,5] provided several such approaches and their modifications for solving quasi-static problems with interface cracks in a way of a cohesive zone model (CZM) [6-7]. Keeping the same variational philosophy [8] with material cracks included to the model generalisation, a damage phase-field model (PFM) [9-11] was considered to simulate such crack growth. These cracks are also called diffuse as, relating them to a scalar material damage variable, represented by at least a continuous function, they seem to be made vague, though the width of their haze can be appropriately controlled.

* Corresponding author: Roman Vodička, E-mail address: roman.vodicka@tuke.sk

Numerical solution for such cracks then comprises some evolution models which naturally incorporates standard time stepping and finite element discretisation. The variational character of the approach then includes optimisation algorithms, too. In the simplest case, the pertinent functionals are considered convex even quadratic for whose minimisation there exist quadratic programming algorithms [12], which can be straightforwardly adapted for the general convex case if applied sequentially [13].

In what follows, we first describe the physical and mathematical model in terms of energies and governing relations for their evolution, and then we show selected aspects of the model discretisation. Finally, we document the behaviour of the proposed approach by a simple numerical test.

2. Physical and mathematical model description

Let us consider a domain Ω which consists of at least two bonded parts as for two such parts Ω^A and Ω^B is shown in Figure 1. The respective boundaries of the parts are denoted Γ^A and Γ^B . The common part of the boundaries, i.e. a contact zone, a stick zone or an interface, is marked Γ_C . Each of the boundaries is additionally split into disjoint parts according to prescribed boundary conditions: Γ_D where displacements u are given by a known function g , and Γ_N where tractions p are supposed to be prescribed by another known function f .

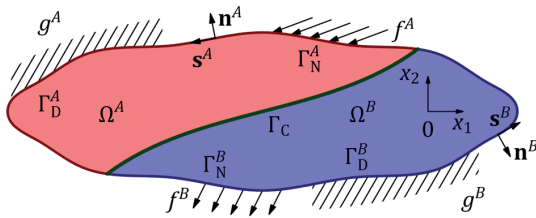


Fig. 1: Description of a domain.

As the boundary conditions change in time, the state of the model, described by its energy state, evolves. This state is described by displacement field u in the interior of the domains, a gap of displacements $\llbracket u \rrbracket$ along interfaces, and two internal parameters α and ζ characterising current damage and varying between 1 and 0: the former parameter pertains to the damage

state derived from the damage PFM in the interior of the domains so that the maximal value $\alpha=1$ corresponds to undamaged state and the minimal value $\alpha=0$ belongs to total damage, meant as a crack. Correspondingly, the latter parameter characterises the state of the interface, considered as a negligibly thin adhesive layer, in the same manner with $\zeta=1$ corresponding to the undamaged adhesive and $\zeta=0$ pertaining to an interface crack along the adhesive. It should be noted that in similar models of other authors the values for damaged and undamaged state may be interchanged, cf. [8,9].

The energy state includes the free energy represented here by the elastic stored energy E of the domain under plane strain conditions and of the interface which may be considered as follows:

$$\begin{aligned} E(t; u, \alpha, \zeta) = & \int_{\Omega} \frac{1}{2} \Phi(\alpha) C e(u) : e(u) + \\ & + \frac{3}{8} G_c \left(\frac{1}{\varepsilon} (1-\alpha) + \varepsilon |\nabla \alpha|^2 \right) dx + \\ & + \int_{\Gamma_C} \frac{1}{2} \varphi(\zeta) (\kappa \llbracket u \rrbracket) \cdot \llbracket u \rrbracket + \\ & + G_c' (1-\zeta) + \frac{1}{2} \kappa_g (\llbracket u \rrbracket_n)^2 ds \end{aligned} \quad (1)$$

for an admissible displacement field u , in the sense that it satisfies the displacement boundary conditions on Γ_D , and admissible damage parameters α and ζ , i.e. their values lying in the interval $[0,1]$. Otherwise, it is considered that the value of E is infinite. The introduced parameters include stiffness matrix C of the material of the domains, initial stiffness κ of the undamaged adhesive layer and the compressive stiffness κ_g to replace standard Signorini contact condition by a normal stiffness penalisation energy term. Further, the energy accumulated due to new crack appearance requires G_c as fracture energy for domain cracks, and G_c' as fracture energy of the interface cracks. The functions $\Phi(\alpha)$, $\varphi(\zeta)$ are degradation functions of the domain (related to a PFM) and interface (related to a CZM), respectively. They determine how the stiffness of the material decreases during the damage process. There are various representations of them in literature which are restricted here to the simplest choices: $\Phi(\alpha) = \left(\frac{\varepsilon^2}{\varepsilon_0^2} + \alpha^2 \right)$, where ε is a characteristic length parameter for the PFM (determining the width of

the diffuse crack), and the parameter ε_0 adjusts residual stiffness after total damage to avoid degeneration of the totally damaged material in the numerical solution. Standardly, the term $\int_{\Gamma_{\text{crack}}} G_c ds$ is used for accumulating energy of the crack in Griffith-like models. Here, it is replaced by a generalised Abrosio-Tortorelli [14] functional (the term containing G_c in Eq. (1)) controlling the evolution of the damage PFM diffuse crack. The interface degradation function is set to $\phi(\zeta) = \zeta^2$, and it modifies the elastic energy of the damageable interface as in the approaches from [4,5] but in a simplified form, in order to have the same form as for the material cracks.

Some energy of the crack formation process is usually dissipated from the system. While in the present model we included it whole into the stored energy, it is still necessary to guarantee a unidirectional character of the damage process at least by the assumption that there is no additional dissipated energy. This can be expressed as a potential $R(\dot{\alpha}, \dot{\zeta}) = 0$, provided that $\dot{\alpha} \leq 0, \dot{\zeta} \leq 0$, otherwise it would be infinite to guarantee impossibility of such a state.

Finally, if there are some external forces, their energy should be added to the system, too. In Figure 1 we considered forces applied at a part of boundary Γ_N , their energy includes the functional

The relations which govern the state evolution

$$F(u) = - \int_{\Gamma_N} f \cdot u ds. \quad (2)$$

can be written in a form of nonlinear variational inclusions with initial conditions (corresponding to an undamaged state)

where ∂ generally denotes a partial subdifferential

$$\begin{aligned} \partial_u E(t; u, \alpha, \zeta) + \partial_u F(u) \ni 0, \quad u|_{t=0} = u_0, \\ \partial_\alpha E(t; u, \alpha, \zeta) + \partial_\alpha R(\dot{\alpha}, \dot{\zeta}) \ni 0, \quad \alpha|_{t=0} = 1, \\ \partial_\zeta E(t; u, \alpha, \zeta) + \partial_\zeta R(\dot{\alpha}, \dot{\zeta}) \ni 0, \quad \zeta|_{t=0} = 1. \end{aligned} \quad (3)$$

as the functionals does not have to be smooth, e.g. R jumps from zero to infinity. For smooth functionals, subdifferentials can be replaced by Gateaux differentials and the inclusions by equations.

3. Notes to the numerical approach

Both, a time stepping algorithm and a spatial discretisation are required for the numerical solution of Eq. (3). The latter is implemented by a standard finite element approach using triangular elements [15] and will not be discussed here. The time discretisation by a semi-implicit fractional-step method, referred also as staggered scheme, relies on separately quadratic character of the proposed energy functional Eq. (1) with respect to each state variable, which then guarantees a variational character of the solved problem.

For the solution, we thus choose a fixed time step τ for a fixed time range $[0, T]$ such that the solution is obtained at the instants $t^k = k\tau$ for $k=1, 2, \dots, T/\tau$ and denoted u^k for displacements and α^k, ζ^k for the damage variables. In order to obtain such an algorithm from Eq. (3), the derivatives in the rate variables are approximated by the finite differences e.g. $\dot{\alpha} \approx \frac{\alpha^k - \alpha^{k-1}}{\tau}$ – the differentiation with respect to the rate is accordingly replaced by differentiation with respect to α^k . These replacements then provide Eq. (3) in the following form:

$$\begin{aligned} \partial_{u^k} E(t^k; u^k, \alpha^{k-1}, \zeta^{k-1}) + \partial_{u^k} F(u^k) \ni 0, \quad u^0 = u_0, \\ \partial_{\alpha^k} E(t^k; u^k, \alpha^k) + \partial_{\alpha^k} R(\alpha^k - \alpha^{k-1}) \ni 0, \quad \alpha^0 = 1, \\ \partial_{\zeta^k} E(t^k; u^k, \zeta^k) + \partial_{\zeta^k} R(\zeta^k - \zeta^{k-1}) \ni 0, \quad \zeta^0 = 1. \end{aligned} \quad (4)$$

The separation of variables in a staggered algorithm then provides two minimisations to be performed at each time step: the first minimisation with respect to the displacements of the functional

$$H_u^k(u) = E(t^k; u, \alpha^{k-1}, \zeta^{k-1}) + F(u) \quad (5)$$

renders u^k as its minimiser (the constraint for u is hidden in the definition of E), and the second minimisation with constraints $0 \leq \alpha \leq \alpha^{k-1}$ and $0 \leq \zeta \leq \zeta^{k-1}$ (the lower bound is hidden in the definition of E , the upper bound comes from R) of the functional

$$H_d^k(\alpha, \zeta) = E(t^k; u^k, \alpha, \zeta) \quad (6)$$

provides ζ^k as the constrained minimiser. These two minimisations are solved repeatedly for $k=1, 2, \dots, T/\tau$. In fact, both functionals are quadratic in the present case so that various quadratic programming algorithms can be used in the numerical solution, see e.g. [12].

4. A computational example

The proposed model will be tested in a simplified problem to demonstrate mutual interaction between an interface and a domain crack.

The geometry of the plane strain deformation state for the example is shown in Figure 2. We consider three mutually bonded blocks, where only one of the interfaces, plotted thicker in the picture, is damageable and thus allowing for cracking. The elastic properties are $E = 20.8 \text{ GPa}$, $\nu = 0.3$ and the fracture energy $G_c = 0.1 \text{ kJm}^{-2}$, while that of the vertical interface is $G_c^I = 1 \text{ Jm}^{-2}$. The cracking along other interfaces is forbidden by setting the fracture energy ultra high. The initial stiffness κ of the damageable interface is 1 TPam^{-1} . The displacement loading $g(t)$ is linearly increasing by the velocity $v_0 = 1 \text{ mms}^{-1}$, where the time steps are chosen 0.1 ms . The mesh size (min.) is $h = 0.2 \text{ mm}$.

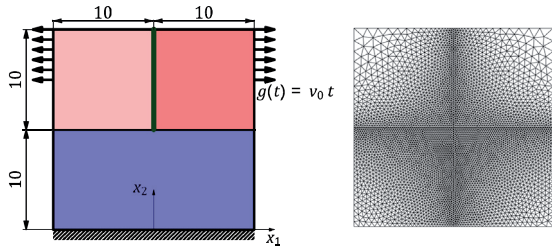


Fig. 2: Geometry for the example with the interface and the material cracks and the used mesh.

The following drawings reveal the character of the fracture process. First, there appears an interface crack, which stops propagating when it reaches the bottom block. The distributions of interface variables, namely the normal stress σ_n and the damage variable ζ , at three selected instants are shown in Figure 3. The damage propagation in the sense of the CZM appears in the region, where ζ lies between the limit values. In the same region, a stress distribution related to the CZM can be observed. The apparent stress maximum at approximately 30 MPa is in accordance with given numerical data, as the model guarantees no interface damage evolution for stress lower than $\sqrt{\kappa G_c^I} = 31.6 \text{ MPa}$, see [4].

Similarly, for the domain damage to initiate an opening crack it is necessary to reach the level $\sqrt{\frac{3KG_c}{2\varepsilon}} = 547.7 \text{ MPa}$, of the critical stress trace σ_{tr} , where K is the bulk modulus, here 20 GPa , and $\varepsilon = 0.01$.

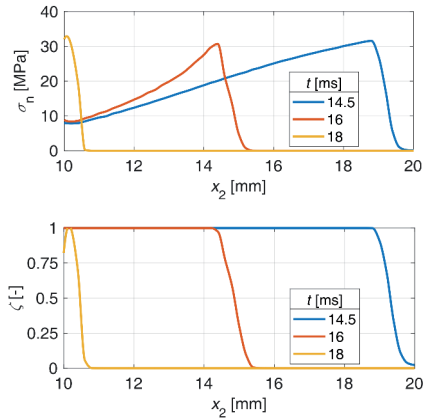


Fig. 3: Interface stress σ_n and interface damage ζ for three instants, where the first instant corresponds to the moment of the interface crack initiation, and the last catches the situation when the interface crack tip approaches the bottom body.

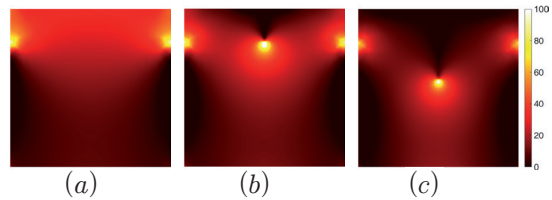


Fig. 4: The stress σ_{tr} distribution in the structure while the interface crack is propagating shown at the same instants $t = 14.5 \text{ ms}$, 16 ms , 18 ms ((a) to (c), respectively) as in Figure 3.

This value is not arrived at while the interface crack is growing as can be seen in Figure 4. All these pictures show the stress trace distribution in the domains at the same instants as used before – its maximum is about 100 MPa close to the (interface) crack tip. Therefore, this crack does not immediately continue to the bottom block, the required energy release rate has not been reached yet. Finally, the deformed structure with an opening crack shown at the same selected instants are shown in Figure 5.

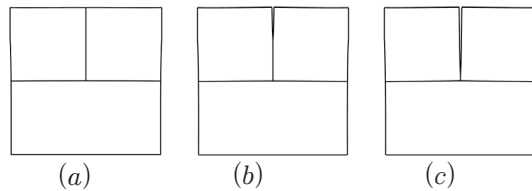


Fig. 5: Crack propagation along the interface with the deformation magnified 8 times. The snapshots belong to the state of the interface crack at $t = 14.5 \text{ ms}$, 16 ms , 18 ms ((a) to (c), respectively), introduced in Figure 3.

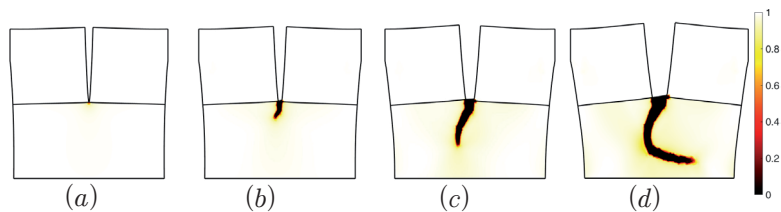


Fig. 6: Crack propagation in the domain, the displacements are magnified 8 times. The snapshots belong to the instants $t = 50$ ms, 80 ms, 130 ms, 190 ms ((a) to (d), respectively), where the first instant again corresponds to material crack initiation. The colour bar displays the state of the damage variable α .

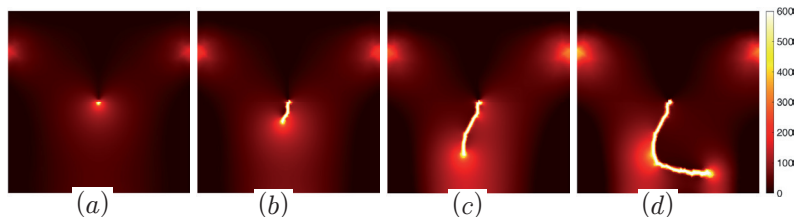


Fig. 7: The stress trace σ_{tr} distribution in the structure while the material crack is propagating, the same instants as in Figure 6: $t = 50$ ms, 80 ms, 130 ms, 190 ms ((a) to (d), respectively).

The continuing crack appears later and is spread in the vertical direction until it approaches the fixed bottom side of the bottom block when it kinks to the more or less horizontal direction. The crack starts growing at the first instant used in Figure 6, the time gap between the last instant from Figure 5 and the first instant from Figure 6 is obvious. The distribution of phase-field damage α obeys the expected behaviour of PFM – it is zero (or near zero) only in a narrow band introduced by the crack. The stress near the crack tip reaches the aforementioned critical value as Figure 7 presents (notice different range for the stress trace in a comparison to Figure 4).

5. Conclusions

A computational model for problems with both interface and domain cracks has been introduced. The model is based on a damage theory and combines interface cracks treated as in cohesive zone models, and material cracks treated as diffuse cracks of phase-field damage. In any case, the degradation of elastic properties may be controlled by appropriately chosen degradation functions, though in this paper only one choice of them has been used.

From the computational point of view, the proposed problem is solved by a staggered modelling scheme, guaranteeing a variational

structure for the numerical approximation to the model. The methods of quadratic programming, and finite elements appeared to be suitable tools for the spatially discretised part of the solution.

Naturally, there are a few parameters in the model which should be appropriately tuned to obtain results which agree with experimental observations. Nevertheless, it is supposed that the present approach turns to be successful also in more complex engineering calculations.

Acknowledgments

The author acknowledges support from the Ministry of Education of the Slovak Republic by the grant VEGA 1/0078/16 and VEGA 1/0374/19.

References and Notes

- [1] Frémond, M. (1985). Dissipation dans l'adhérence des solides. *Comptes Rendus de l'Académie des Sciences – Series II* 300:709–714.
- [2] Maugin, G.A. (2015). The saga of internal variables of state in continuum thermo-mechanics. *Mechanics Research Communications*, 69, 79–86.
- [3] Vodička, R., Mamtič, V., Roubíček, T. (2014). Energetic versus maximally dissipative local solutions of a quasi-static rate-independent mixed-mode delamination model. *Meccanica*, 49, 2933–2963.
- [4] Vodička, R. (2016). A quasi-static interface damage model with cohesive cracks: SQP-SGBEM implementation. *Engi-*

- neering Analysis with Boundary Elements, 62, 123-140.
- [5] Vodička, R., Mantič, V. (2017). An energy-based formulation of a quasi-static interface damage model with a multilinear cohesive law. *Discrete and Continuous Dynamical Systems — Series S*, 10(6), 1539-1561.
 - [6] Ortiz, M., Pandolfi A. (1999). Finite-deformation irreversible cohesive elements for three-dimensional crack propagation analysis. *International Journal for Numerical Methods in Engineering*, 44, 1267-83.
 - [7] Park, K., Paulino, G.H. (2011). Cohesive zone models: a critical review of traction-separation relationships across fracture surfaces. *Applied Mechanics Review*, 64, 6, 061002.
 - [8] Bourdin, B., Francfort, G.A., Marigo, J.J. (2008). The variational approach to fracture. *Journal of Elasticity*, 91, 5-148.
 - [9] Miehe, C., Hofacker, M., Welschinger, F. (2010). A phase field model for rate-independent crack propagation: Robust algorithmic implementation based on operator splits. *Computer Methods in Applied Mechanics and Engineering*, 199, 2765-2778.
 - [10] Tanné, E., Li, T., Bourdin, B., Marigo, J.J., Maurini, C., (2018). Crack nucleation in variational phase-field models of brittle fracture. *Journal of the Mechanics and Physics of Solids*, 110, 80-99.
 - [11] Paggi, M., Reinoso, J., (2017), Revisiting the problem of a crack impinging on an interface: A modeling framework for the interaction between the phase field approach for brittle fracture and the interface cohesive zone model *Computer Methods in Applied Mechanics and Engineering*, 321, 145-172.
 - [12] Dostál, Z. (2009). *Optimal Quadratic Programming Algorithms*. Springer Optimization and Its Applications. Springer, New York.
 - [13] Nocedal, J., Wright, S. (2006). *Numerical Optimization*, Springer, New York.
 - [14] Ambrosio, L., Tortorelli, V.M. (1990). Approximation of functional depending on jumps by elliptic functional via C-convergence. *Communications in Pure and Applied Mathematics*, 43, 999-1036.
 - [15] Zienkiewicz, O.C., Taylor, R, Zhu, J.Z. (2013). *The Finite Element Method: Its Basis and Fundamentals*, 7th Edition, Butterworth-Heinemann, Oxford, UK.

